The Duration of Non-flow Periods Influences the Dynamic Responses of Biofilm Metabolic Activities to Flow Wewetting

Lingzhan Miao[1], Chaoran Li[1], Tanveer M. Adyel[2], Zhilin Liu[1], Jun Wu[1], Songqi Liu[1], Wanyi Li[1], Jun Hou*[1]

[1]Key Laboratory of Integrated Regulation and Resources Development on Shallow Lakes, Ministry of Education, College of Environment, Hohai University, Nanjing, People's Republic of China, 210098

[2]Centre for Integrative Ecology, School of Life and Environmental Sciences, Deakin University, Melbourne, VIC 3125, Australia

*Corresponding author:

Professor Jun Hou, Tel.: +86-25-83787930; fax: +86-25-83787930.

Author affiliation: Xikang Road 1st, Nanjing, People's Republic of China, 210098

E-mail: hhuhjyhj@126.com; hjy_hj@hhu.edu.cn

Key Points:

- Distinct dynamic responses of biofilm metabolism were observed from short-term and long-term desiccation treatments to the flow rewetting.
- Most of the functional index of biofilms in short-term desiccation were recovered to that of the control level after 20 days of rewetting.
- Prolonged desiccation led to irreparable damage to biofilm metabolic functions and the selectivity of carbon metabolism after rewetting.

- Graphical Abstract

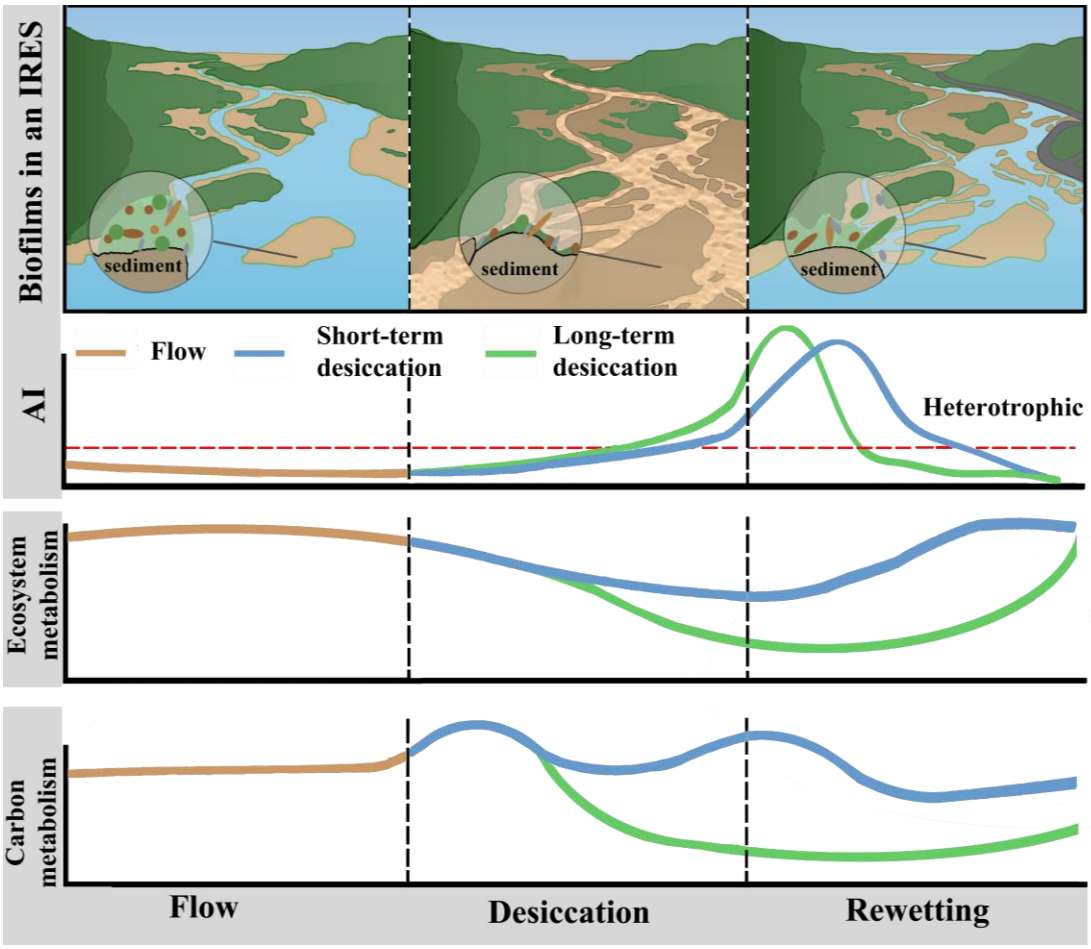

Abstract

Global change has led to the increased duration and frequency of droughts and may affect the microbial-mediated biochemical processes of intermittent rivers and ephemeral streams (IRES). Effects of flow desiccation on the physical structure and community structure of benthic biofilms of IRES have been addressed, however the dynamic responses of biofilm functions related to ecosystem processes during the dry-wet transition remain poorly understood. Herein, dynamic changes in biofilm metabolic activities were investigated during short-term (25-day) and long-term (90-day) desiccation, both followed by a 20-day rewetting period. Distinct response patterns of biofilm metabolism were observed based on flow conditions. Specifically, biofilms were completely desiccated after 10 days of drying. Biofilm ecosystem metabolism, represented by the ratio of gross primary production (GPP) and community respiration (CR), was significantly inhibited during desiccation and gradually recovered back to autotrophic after rewetting due to the high resilience of GPP. Also, the potential metabolic activities of biofilms were maintained during desiccation and showed a tendency to recover after rewetting. While long-term desiccation caused irreparable damage to the total carbon metabolism of biofilms that could not be recovered to the control level even after 20 days of rewetting. Moreover, the metabolic activities of amine and amino acids showed an inconsistent pattern of recovery with total carbon metabolism, indicating the development of selective carbon metabolism. This research provides direct evidence that the increased non-flow periods affects biofilm-mediated carbon biogeochemical processes, which should be taken into consideration for the decision-making of the ecological and environmental flow of IRES.

Keywords: Biofilm; intermittent rivers and ephemeral streams; microbial functions; dynamic responses; carbon metabolism

1 Introduction

Global climate variabilities and human activities have led to the increasing intermittency of numerous streams and rivers (Acuña et al., 2014 , Messager et al., 2021). Intermittent rivers and ephemeral streams (IRES) are characterized by the alternation of desiccation and rewetting hydrological phases, contributing to the biodiversity and biogeochemical processes (Lv et al., 2017), and functional integrity of fluvial systems (Shumilova et al., 2019, Messager et al., 2021). However, the increasing flow intermittency has lead to a harsh environment for the aquatic organisms, especially the microbial communities, and influences the ecosystem processes ongoing in the IRES (Navarro-Ortega et al., 2015). for instance, benthic biofilms serve as an ecological indicator for coupling the structure and function of the river ecosystem and play a key driving role in the primary production, nutrient circulation, and energy flow of the river system (Sun et al., 2021 , Fan et al., 2021). However, unpredictable desiccation may affect the community structure and function of biofilm, which in turn influence the ecosystem processes of the IRES ecosystem (Bogan et al., 2017, Zlatanović et al., 2018).

Previous studies have demonstrated that the duration, frequency, and severity of the dehydration could affect the physicochemical properties, community composition, and activities of enzymes in biofilms of aquatic system (Sabater et al., 2016 , Shumilova et al., 2019). For example, the alternation of desiccation and rewetting hydrological phases has the greatest influence on the algal community, followed by bacterial, and the least influence on the fungal

community in biofilms(Gionchetta et al., 2019). The increasing desiccation periods are reported to extend the ecological niche, and significantly increase the β-diversity of biofilm communities (Feng et al., 2020), while the α-diversity (species richness) decreased significantly in most biofilm communities(Sabater et al., 2016 , Zlatanović et al., 2018). Also, the combination of the temporal components and the severity of the desiccation affected the microbial function of biofilm(Colls et al., 2019), leading to a reduction of extracellular enzymes(Timoner et al., 2012 , Colls et al., 2019), and promoting biofilm to be more heterotrophy(Acuña et al., 2015). Moreover, several recent studies have shown that the increasing desiccation period and intensity affect the recovery of microbial community structure(Pohlon et al., 2018) and the ecosystem metabolism, the ratio of gross primary production (GPP) and community respiration (CR), of biofilms(Acuña et al., 2015). Due to the importance in ecosystem processes of biofilm functions, recovery of biofilm microbial functions following desiccation should be further considered.

However, most previous studies investigated the recovery of the community structure and integrated functions of biofilms after a predetermined experimental cycle, little is known about the dynamic responses of biofilm metabolic activities over time under such conditions. Due to the intrinsic resistance and physiological recovery of biofilm under disturbance (Steven et al., 2021), the question here is whether the microbial function of biofilms can be maintained during the desiccation and then can be recovered to original state after flow rewetting. If so, how long does biofilms take for the function to achieve stability, and this question is related to that whether the setting of the recovery period of biofilms after desiccation in previous studies is reasonable (5-10 days; (Fabian et al., 2018 , Gionchetta et al., 2019 , Shumilova et al., 2019)). More importantly, the ecological indicators, such as GPP, CR, and autotrophic index (AI) used in previous studies can only reflect the integrated functions of biofilms, more detailed indicators (for example, carbon metabolism determined by Biology Eco) should be applied to explore the dynamic responses of biofilm metabolic activities to dry and wet stress in IRES systems.

In this study, we aimed to identify the effects of the duration of non-flow periods on the dynamic responses of biofilm microbial functions during the alternation of desiccation and rewetting conditions through indoor simulation experiments. Two desiccation periods (short-term (25-day) and long-term (90-day) of biofilms were performed and both followed by a 20-day rewetting period. During the whole experimental period, indicators of biofilm integrated functions were identified, including AI and ecosystem metabolism (represented by GPP and CR ratio). In addition, Biolog eco was used to provide more detailed information about biofilm carbon metabolisms, such as specific activities of carbon sources and functional diversity. We hypothesized that the response patterns of the integrated indicators (AI and ecosystem metabolism) and carbon metabolism may be different after longer desiccation, changes of different metabolic activities may be consistent in desiccation (i); the recovery rate of biofilm functions in the rewetting period after long-term desiccation should be lower than that after short-term desiccation (ii); and the metabolic activity of biofilm could be restored by rewetting after short-term desiccation, but not after long-term desiccation(iii).

2 Materials and Methods

2.1 Biofilm inoculation

The biofilm inoculation experiment was designed according to our previous study (Miao et al., 2020). The cultivation device for the sample was located at the Qin Huai River in Nanjing,

Eastern China. All incubation devices were secured to a depth of 50 cm to recieve the same light output and intensity. Each device was cultured for 44 days (from 30 October 2020 to 7 December 2020) to obtain mature biofilm (Wu et al., 2014 , Battin et al., 2016). Water quality in the Qin Huai River was measured over the culture period (Table S1). The experimental devices with all cobblestones and river water in the cultivation station were taken to the lab for further experiment.

2. 2 Laboratory experiment design

Flowing artificial water tanks (160 cm long, 20 cm wide, and 30 cm high) were designed for indoor adaptation of mature biofilms in a greenhouse at 18±2 ℃ with natural light. The tanks were equipped with a pump to modify the water conditions (Figure S1). The flow rate in our culturing device was kept at 0.014 m/s controlled by a pump (BT100-1L, China) to create favorable conditions for biofilm adaptation (Liao et al., 2018).

In the laboratory experiment, 5ml/L nutrient solution/water (Table S2) was added weekly to the water tank for the adaptation of biofilms(Hou et al., 2019). After 2 weeks of adaptations, all cobblestones with biofilm were distributed in three parts. One-third of the cobblestones were kept in the tank with water as a control group, and one-third of the cobblestones were transferred to another tank for 25 days of desiccation and subsequent rewetting; as well the rest of the third was transferred to another tank for 90 days of desiccation and subsequent rewetting.

The selected duration of the non-flow periods fall within the range for the non-flow period reported for other IRES and artificial streams (20~100 days) (Fazi et al., 2013) (Acuña et al., 2015). Herein, 25 days of desiccation with 20 days of rewetting (expressed as 25-Rewetting) and desiccation for 90 days with 20 days of rewetting (expressed as 90-Rewetting) were conducted in the alternation of desiccation and rewetting experiments (Figure 1). Before desiccation, surface and free pore water were drained from the experimental tanks following the precudures in previous study (Zlatanović et al., 2018). After drying, the re-equipment of the biofilm was carried out by ascending reconstruction of small flows, avoiding destroy the biofilm on the surface of the cobblestones. Then, the water column was filled to the control level using the pump (Zlatanović et al., 2018). Samples were taken between the control group and the experimental group on days 0, 1, 3, 5, 7, 10, 25, and 90 of the non-flow periods, and in the experimental group on days 1, 3, 5, 7, 10, and 20 of the rewetting periods to measure various indicator variables (Table S3). At each sampling time, the pump was stopped, and a sterile brush and tweezers were used to collect the biofilms from the cobblestone surfaces (Liao et al., 2018, Liao et al., 2019).

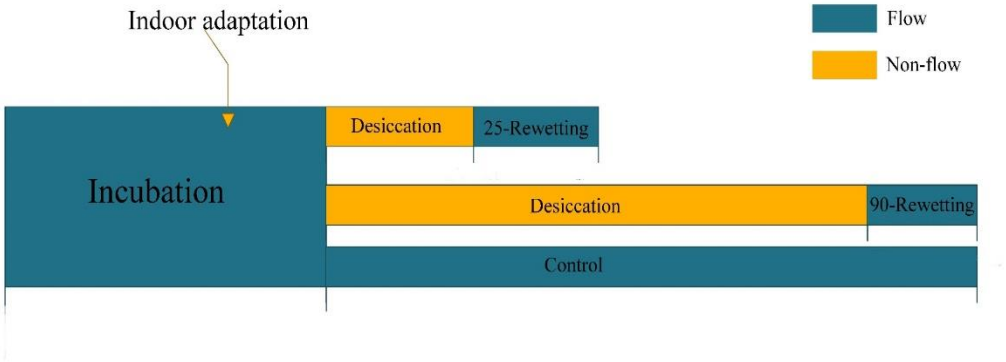

Figure 1. The alternation of desiccation and rewetting experiment time axis.

149 2.3 The biomass and morphology of biofilm

150 The biomass of biofilms, represented by ash-free dry weight (AFDW) was measured per
151 given area (30cm^2, 10-15 cobblestones). Biofilm samples were dried at 105 ℃ for 24 hrs and
152 then calcined at 450 ℃ for 4 hrs to estimate AFDW (Timoner et al., 2012).

153 Biofilm sample morphology was observed using an ESEM (QUANTA200, FEI
154 Company, The Netherlands) at various hydrologic stages(Yurudu, 2012). The biofilms on
155 cobblestones were attached to the sampling table with conductive adhesive, then placed in the
156 electron microscope sampling room and vacuumed and photographed in selected positions.

157 2.4 Characterization of the indicators of integrated function

158 This study identified indicators for the integrated function of biofilms, including GPP,
159 CR, and AI.

160 The AI is defined as the ratio AFDW/chl-a, which can reflect the shifts in dominance of
161 functional groups (i.e., AI>200 indicates a high proportion of heterotrophic) (Delgado et al.,
162 2017). The chlorophyll content of biofilm was determined with a portable pulse amplitude-
163 modulated fluorometer (PGYTO-PAM; WALZ, Effeltrich, Germany) (Hou et al., 2019,
164 Schreiber et al., 2002).

165 Ecosystem metabolism governs the fixation and mineralization of organic carbon (C) in
166 streams and is quantitatively expressed by the GPP: CR ratio (Schreiber et al., 2002). We
167 followed the approach from previous studies (Acuña et al., 2008) to estimate the biofilm
168 metabolism from the drop and rise in dissolved oxygen concentration, which was widely used in
169 ecosystem metabolism studies in rivers and streams (Gómez-Gener et al., 2016 , Bott et al.,
170 1997). We used square recirculating chambers (24cm long, 19cm wide, 18cm high) to estimate
171 biofilm oxygen production and consumption(Bott et al., 1997). The chambers were equipped
172 with a submersible pump that recirculated water, avoiding the generation of low diffusion areas
173 within the chamber. The CR and GPP were measured for 120 minutes in constant dark and
174 brightness conditions, respectively. Dissolved oxygen was recorded at 10-min intervals with
175 oxygen sensors (miniDO2T Logger, PME, USA) (Liu et al., 2020, Adyel et al., 2017). Metabolic
176 rates were calculated as described by ACUÑA and others(Acuña et al., 2008 , Zlatanović et al.,
177 2018). The GPP and CR were calculated as Eq. (1-2).

178 $$CR = \left(\frac{dC_{treatment}}{dt}\right)_{night} * \left(\frac{V_{water}}{A_{sed}}\right) \quad (1)$$

179 $$GPP = \left(\frac{dC_{treatment}}{dt}\right)_{day} * \left(\frac{V_{water}}{A_{sed}}\right) \quad (2)$$

180 where $C_{treatment}$ is oxygen (mg/L), t is time(h), night and day represent the dissolved O_2
181 concentration data set used in the dark treatment and light treatment conditions (the measurement
182 time is 120 min), V_{water} is the total water volume (L) in the metabolism chamber, and A_{sed} is the
183 measuring bed surface(m^2) (Zlatanović et al., 2018).

184 Based on the measurement of CR and GPP, the resistance and resilience of biofilms
185 during the experimental period were also calculated (Acuña et al., 2015). Resistance served as an
186 indicator of the capacity of stabilization and was calculated as the % decline in the variable
187 experienced between the last measurement before a disturbance and the first measurement after
188 the condition was restored. The resilience of biofilm was determined as the slope of the linear

functions of the relationship between each of the response variables and the time when flow resume.

2.5 Carbon metabolism of biofilms

Biofilm samples from different hydrological stages were collected to determine their carbon metabolic activities using Biolog Eco Plates (Biolog Inc., Hayward, CA, USA) (Zak et al., 1994). The experimental methods are detailed in our previous study and given in the Supplementary Information (Miao et al., 2021).

Based on the measured AWCD of Biolog Eco plate when biofilm metabolism is stable (120h), the carbon metabolic functional diversity of biofilms were determined and represented by three indices, Shannon-Wiener diversity index (H`), Simpson diversity index (D), and Pielou evenness index (E) (Ge et al., 2018 , Miao et al., 2019), and the formulas are presented in Supplementary Information. At the same time, NMDS analysis was carried out based on different measured values of 31 carbon sources when they reached metabolic stability (120h) in each experimental cycle (Control, Desiccation, 25-Rewetting, and 90-Rewetting). The analytical methodology can be found in the Statistical Analysis section.

2.6 Statistical analysis

All biochemical analyses of the biofilm samples during the desiccation and rewetting were performed in triplicate, and the values are presented as the mean ± standard deviation. A further one-way ANOVA with ecological variables (AWCD or GPP and so on) was used to test for significant differences. T-TEST analyzed the results of the control group and the desiccation group. Graphs were plotted using Origin (Version 2018, Northampton, MA, USA).

Based on Bray-Curtis dissimilarities, NMDS analysis were used to study differences in microbial functional composition in different treatments (Fasching et al., 2020). Then, an ANOVA (permutational multivariate analysis of variance (PERMANOVA) was completed using the Adonis function in the R Vegan package; (Oksanen et al., 2012). An analysis of carbon metabolic diversity data was performed using the statistical environment R (R Core Team 2017) and the packages ggpolt2, ggsignif, and ggpubr(Wickham, 2009, Ahlmann-Eltze, 2019 , Kassambara, 2020).

3 Results

3.1 The water content and micromorphology of biofilms

During the alternation of desiccation and rewetting experiments, the water content of biofilm was shown in Figure S2. After the desiccation started, the water content of biofilm decreased quickly and was completely dehydrated 10 days later. When rewetting begins, the water content of biofilm was rapidly resumed within the first two days, and reached the control level after 10 days of recovery (t-test, $P>0.05$), regardless of the duration of non-flow periods (25 days and 90 days).

The changes in morphology and structure of biofilm were introduced (Figure 2). The micromorphological heterogeneity of biofilm is shown in the images of different map points. With the increase of desiccant content, the phenomenon of disintegration of 3D structure and the

structural fragmentation of biofilm increases gradually (Figure 2a-e), leading to reduced the material transport channels of biofilm. As the rewetting begins, the fragmentation was gradually restored and the 3D structure of biofilms appears to be recovered (Figure 2f-k).

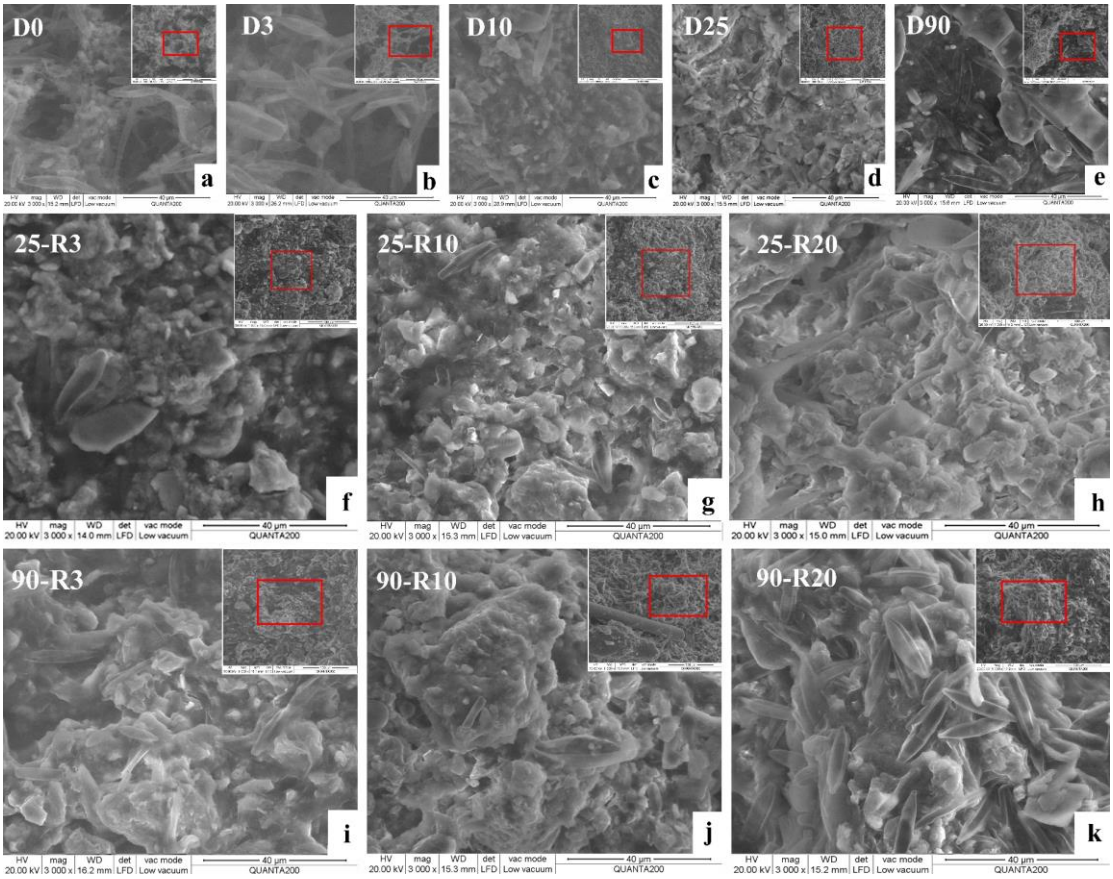

Figure 2. ESEM of biofilm during alternation of desiccation and rewetting. Each image is a detailed image in the red box at the top right. D0 is day 0 of desiccation and R0 is day 0 of rewetting.

3.2 Biomass of biofilm

The AFDW of biofilm decreased rapidly with desiccation time and remained at the range of 0.986 and 1.433 mgcm^{-2} after 7 days of desiccation, significantly different from that of control (t-test, p=0.000169; Figure S3a). The AFDW of biofilm recovered rapidly during rewetting and stabilized after 5 days (Figure S3b,c). While, the AFDW of biofilm can be restored to the control level for the 25-Rewetting group (Figure S3b), not for the 90-Rewetting group (Figure S3c).

With desiccation, chl-a concentration also decreased, and after 7 days, when the biofilm was completely dehydrated, it tended to be close to 0 mg/cm^2 (Figure S3d). Then, as the rewetting progressed, chl-a concentration was restored to 0.06 mg/cm^2 (close to the initial level, t-test, p>0.05) after 10 days (Figure S3e,f). In addition, chl-a content of the biofilm could reach a control level on the seventh day after longer desiccation but did not reach stability during the 20-day rewetting period.

3.3 Changes of the integrated function of biofilms

During desiccation, the value of AI increased with the duration of time, exceeding 200 after 7 days (Figure 3a). This indicated a high proportion of heterotrophic in the biofilm system. When the rewetting started, the AI value raised significantly and then decreased rapidly as rewetting progresses, remaining below 200 after 3 days of rewetting (Figure. 3b,c). In addition, no matter the duration of desiccation, the AI was both recovered to the control level after 20 days of rewetting (t-test, $p>0.05$, Figure 3b,c), indicating recovery of flow promoted autotrophy of biofilms.

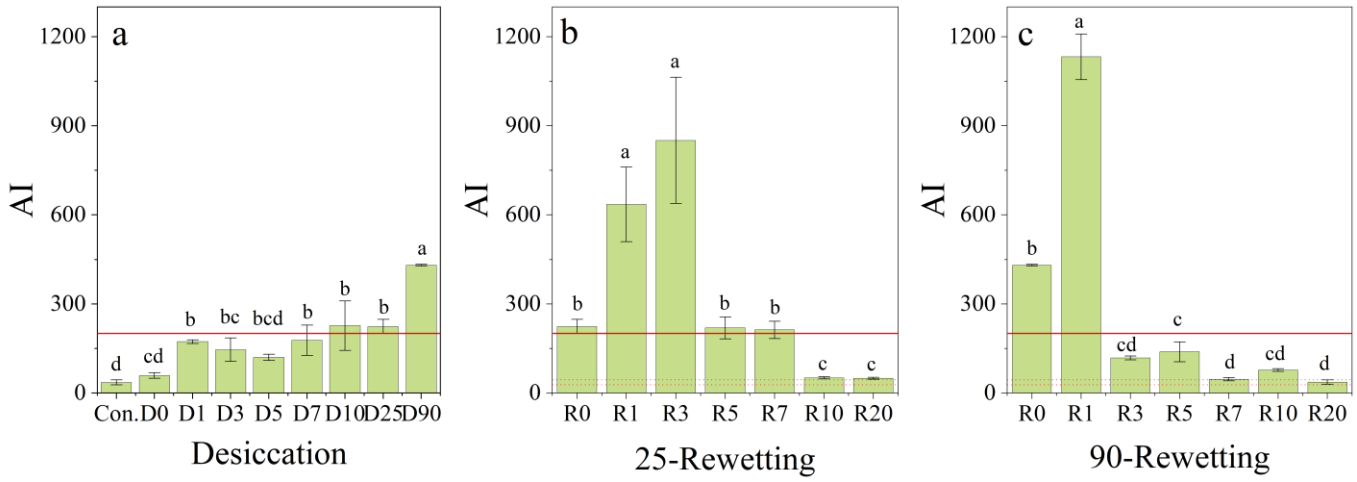

Figure 3. The value of AI (a-c) of biofilm during alternation of desiccation and rewetting. The lines at AI value 200 (a, b, and c) indicate a high proportion of heterotrophic in the biofilm. The dotted lower and upper lines indicate the range of values for the control group(b, c). The error bars indicate standard deviation between parallel samples. The albaphtical letters abc indicate significant differences between samples.

As shown in Figure S4, CR and GPP decreased gradually as the desiccation time increased (Figure S4 a,d), which was consistent with previous studies (Acuña et al., 2015, Zlatanović et al., 2018, Colls et al., 2019). The resistance of biofilms to desiccation was also calculated, as shown in Figure 4d. The resistance of CR has decreased significantly within the first 10 days of desiccation and then stabilized at $67.22 \pm 8.7\%$. The resistance of GPP was observed to continue declining, reaching nearly 0 after 90 days of desiccation. After longer desiccation, resistance to GPP continued to decrease, resulting in a significant decrease in GPP:CR (Figure 4a). The ecosystem metabolism of biofilm changed to heterotrophic metabolism. At the same time, there were differences in the best fitting models of the perturbation response of ecosystem metabolism (Figure 4d). The response of resistance to GPP was better described by an exponential curve with three parameters and X2 ($r^2= 0.97326$), while CR was better described by a sigmoid logistic curve with four parameters ($r^2= 0.99931$), a sign of its ecological threshold in the disturbance-response relationship (Acuña et al., 2015).

After further rewetting, CR gradually recovered to stable levels of control after 10 days (Figure S4b,c). Note that CR had a “brich effect” on the first day of the 90-Rewetting group (Figure S4) (Sabater et al., 2016, Muñoz et al., 2018). At higher resilience (Figure 4e), GPP increased with the prolongation of the rewetting cycle, however, at the end of the 20-day rewetting experiment, it had not yet reached stability (Figure S5e,f). There was no obvious pattern of the change of resilience in the rewetting experiment (Figure 4e). From the point of view of average resilience, the average resilience of GPP of biofilm decreased from 0.173 to

0.130 after longer desiccation (Figure 4e). Conversely, the average resilience of CR was from 0.0522 and increased to 0.0856 (Figure 4e). The average resilience of GPP was always higher than that of CR.

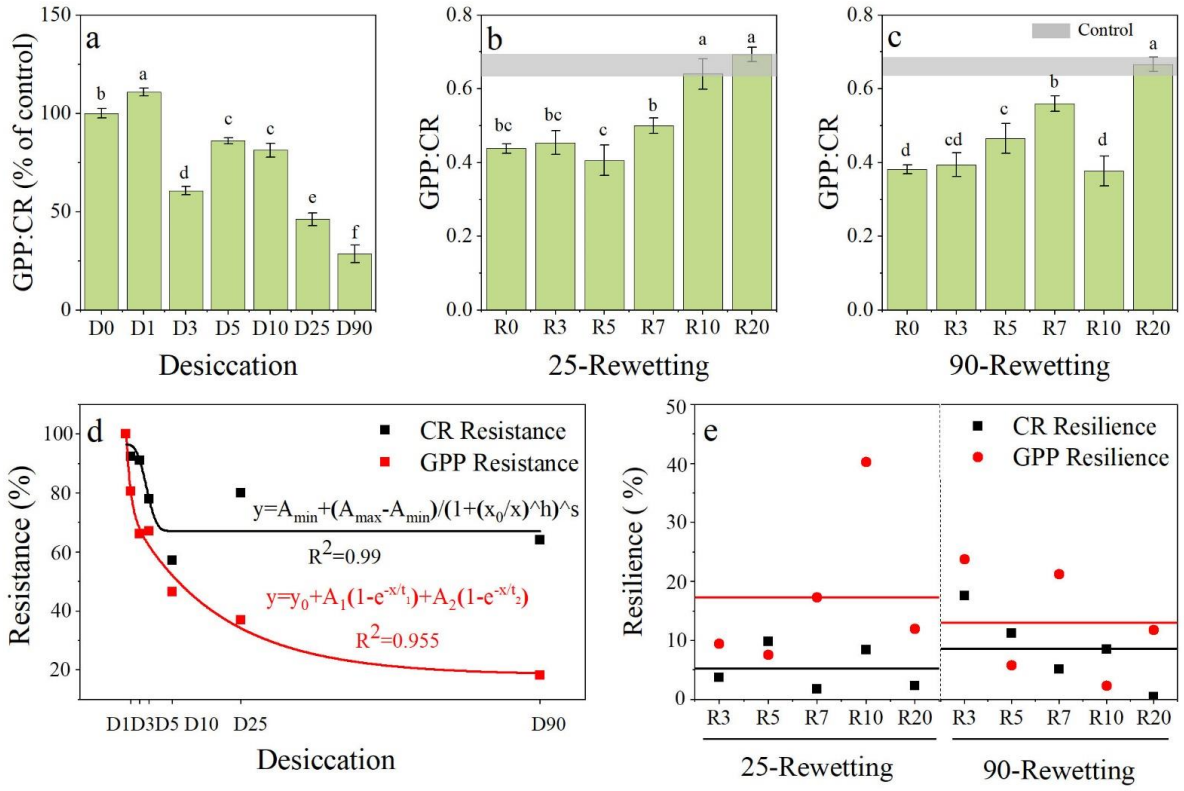

Figure 4. The ecosystem metabolism (represent by the ratio of GPP and CR, a-c) and the resistance of GPP and CR during desiccation (d), and the resilience of GPP and CR after rewetting (e). The shaded grey panels in b and c indicate control. The error bars indicate standard deviation between parallel samples. The albaphtical letters abc indicate significant differences between samples.

3.4 The potential activity of carbon metabolism of biofilms

3.4.1 Effects of desiccation on the carbon metabolism of biofilms

During desiccation, the total AWCD value of biofilms decreased significantly at the beginning (t-test, $p<0.05$) and then fluctuated steadily on the control level before the complete drought (t-test, $p>0.05$) (Figure 5a). The potential activity of biofilm carbon metabolism decreased significantly lower than that of the control group (t-test, $p<0.05$) after the biofilm was the complete drought (Figure 5a).

To evaluate the biofilm metabolic functions in a physiologically relevant approach, 31 carbon sources were classified into six categories, including carbohydrates, amino acids, polymers, amines, carboxylic acids, and miscellaneous. Similar response patterns with the total AWCD were observed in the polymers, carbohydrates, amino acids, and carboxylic acids during desiccation (Figure S5a-d). Different response patterns were observed in the metabolism of

amines and miscellaneous (Figure 5b,c, and Figure S5e,f), with a significant increase in the two carbon species during the first week of desiccation, followed by significant reductions (t-test, $p<0.01$, Figure 5b,c, and Figure S5e,f). The carbon consumption selectivity of biofilm communities during the desiccation process is explained by the difference in the utilization ratio of different carbon sources (Miao et al., 2021).

The results of the Shannon-Wiener diversity index (H`), Simpson diversity index (D), and Pielou evenness index (E) of dynamic changes during desiccation are shown in Table S4. The metabolic function diversity index showed a significant increase (t-test, P-value<0.05) with the desiccation period (Table S4). The high index indicated that desiccation promoted the metabolic functional diversity of biofilm.

3.4.2 Effects of rewetting on the carbon metabolism of biofilms

The dynamic changes of the total AWCD values during the rewetting experiment are shown in Figure 5d,g. The same response patterns were observed in both processes, regardless of the desiccation period (Figure 5d,g). During the first three days of the rewetting experiment, the total AWCD value increased significantly and then fluctuated steadily (Figure 5d,g). The difference here was that the biofilm stabilizes at the control level after 25 days of desiccation and did not return to control after a longer desiccation period (Figure 5d, g). As for the different carbon source specials of biofilms during the rewetting experiments, similar response patterns with the total AWCD were observed for polymers, carbohydrates, miscellaneous, and carboxylic acids (Figure S6a-d and Figure S7a-d). The metabolic response patterns of six different carbon sources after long desiccation were more consistent with those of the total carbon source (Figure S7a-d) as the total metabolic rate. The utilization of miscellaneous remained at the lowest levels, indicating the selective carbon consumption of biofilm communities (Figure S6c and Figure S7c) (Miao et al., 2021).

The metabolic functional diversity index did not show a significant difference at different rewetting times (Table S5 and Table S6). It is noteworthy that the Shannon-Weiner diversity index decreased significantly with the recovery of flow in group 25-Rewetting. Low index suggested that rewetting reduced the metabolic function diversity of biofilms (ANOVA, P-value <0.01).

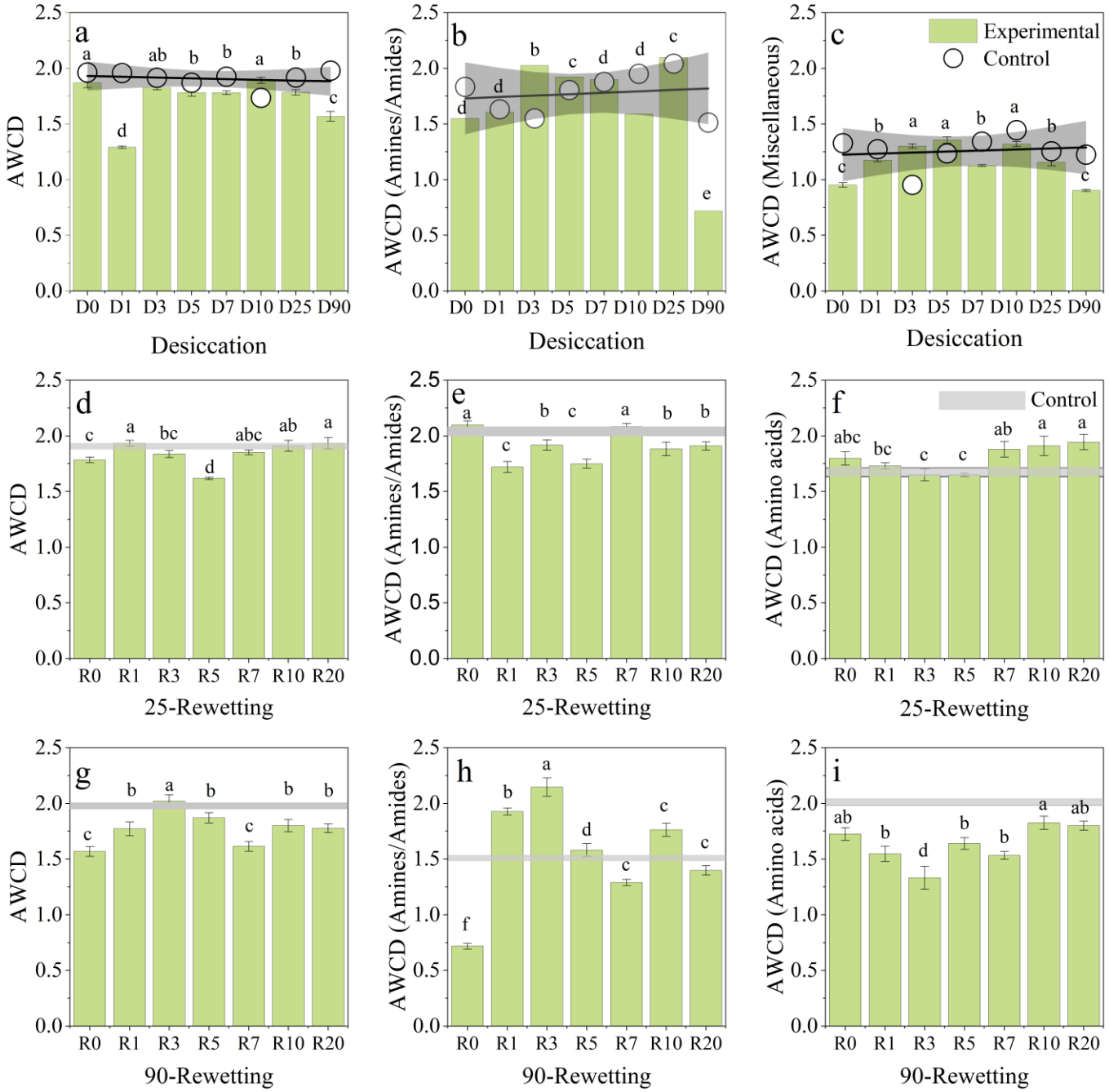

Figure 5. The total AWCD of biofilm (a, d, g) and specific carbon sources that differ from the overall pattern of metabolism (b, c, e, f, h, i) during the alternation of desiccation and rewetting. Linerar fits of control data (a, b, c) indicate 95% confidential level. The shaded grey panels (d, e, f, g, h, i) indicate control. The error bars indicate standard deviation between parallel samples. The albaphtical letters abc indicate significant differences between samples.

3.4.3 Effects of drought duration on carbon source utilization diversity

Microbial functions differed significantly between the 90-Rewetting group with other experimental stages (ANOVA using distance matrices, Bray-Curtis dissimilarity, $p<0.05$, Figure

6a), while there was no significant difference between the 25-Rewetting group and the Control group (ANOVA using distance matrices, Bray-Curtis dissimilarity, $p>0.05$, Figure 6a). The Shannon Diversity Index and the Simpson Diversity Index also showed that short-term desiccation had a reversible effect on biofilm metabolic diversity, while long-term desiccation could not (Figure 6b,c).

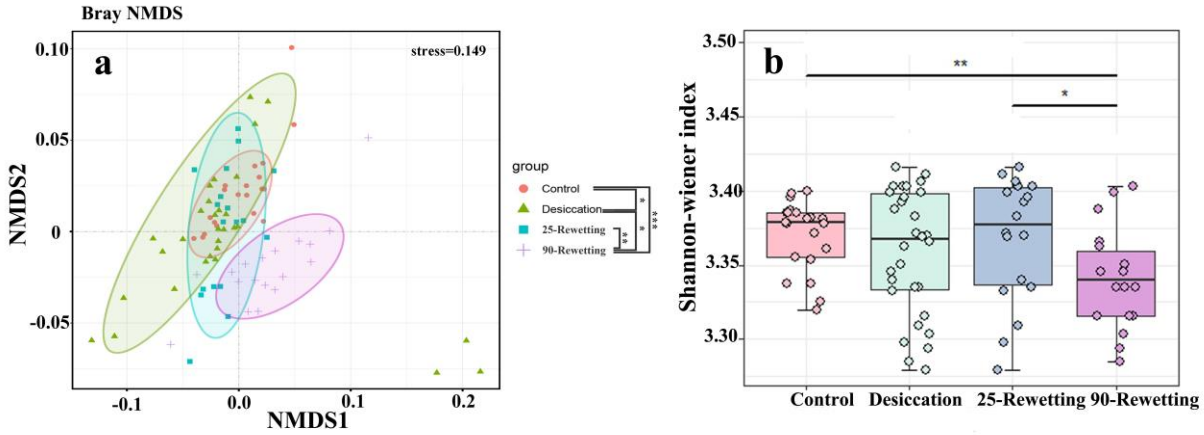

Figure 6. Non-metric multidimensional scaling (NMDS) of all carbon sources (n=31) across experimental stages (Control, Desiccation, 25-Rewetting, 90-Rewetting) (a). Functional diversity of biofilms as the Shannon-wiener index (b) across the experimental stages (* $p < 0.05$, ** $p < 0.01$).

4 Discussion

In this study, the effects of different non-flow periods on the dynamic responses to flow recovery of biofilm metabolic activity were studied using biomass, integrated function indicators (AI and GPP:CR), and carbon metabolic activities. The first thing to be noted that the results of indoor simulation experiments should be carefully extrapolated to the field conditions. Although the irrelevant variables (light, temperature, and organic matters) during the desiccation can be eliminated through such controlled experiments, the disadvantage is that the environmental changes in natural waters are potentially more extreme and stressors can co-occur (Colls et al., 2019, Acuña et al., 2015).

4.1 Response patterns of the biomass and integrated function indicators of biofilm

The results showed that desiccation had a significant effect on the physical structure and biomass of biofilms, and biofilms were completely dehydrated after 10 days. Then, when the rewetting began, the water content, biomass, and micromorphology of biofilms responded rapidly (5-7 days). Regardless of how long the desiccation lasted, they can be returned to the control level (Timoner et al., 2012).

Different response patterns were observed for these two integrated function indicators. In the desiccation experiments, AI increased gradually to over 200, and GPPP:CR decreased gradually, indicating that the increase of the desiccation period would cause severe damage to the autotrophic group and promote heterotrophy of biofilms, consistent with previous studies (Acuña et al., 2015, Delgado et al., 2017). Decreases in AI values and increases in GPP:CR

values in rewetting experiments indicate that the major functional groups in the biofilms are moving to the autotrophic group (Acuña et al., 2015). The dormancy mechanism of algae and an increase in ambient temperature may partly explain why the recovery rate after 90 days of desiccation is faster than after 25 days, contrary to our hypothesis that the response rate of rewetting after 90 days desiccation is lower than that after 25 days.

Different disturbance-response relationships of GPP and CR during the desiccation and rewetting were confirmed by different resistance and resilience of biofilm GPP and CR to flow desiccation and flow recovery. The resistance of biofilm GPP was always lower than that of CR, resulting in a continuous decrease in GPP:CR during desiccation, consistent with previous studies (Timoner et al., 2012 , Acuña et al., 2015). During the rewetting process, the average resilience of the GPP was higher than that of CR, so that the ecosystem metabolism was gradually restored and converted to an autotrophic body. In addition, the GPP disturbance-response relationship was exponent while the relationship was sigmoid for CR, suggesting that flow desiccation exhibit an immediate effect on autotrophs while the effect on heterotrophs was delayed.

Timoner reports that the mechanism of rapid recovery of autotrophic groups from rewetting may be related to the physiological restoration of dry algae and cyanobacteria that remain on the surface of cobblestones(Timoner et al., 2012). So, the increase of effects of duration and severity of the desiccation period may cause more damage to the recovery mechanism, causing the decrease of the average resilience of GPP after long-term desiccation (Figure 4e). The recovery mechanism of heterotrophic taxa may be the accumulation of organic matter (dissolved or granular organic carbon) on the riverbed and in the biofilm during desiccation, which may facilitate rapid respiration after rewetting (Colls et al., 2019). Therefore, the accumulation of organic matter on the river bed increases with the prolongation of the desiccation period, which may lead to an increase in the average resilience of CR after 90 days of desiccation (Figure 4e). Besides, the enhanced CR on the first day of rewetting (Figure S4c) resembles the “birch effect” (pulse of respiration on rewetting a dry soil), which may significantly influence the carbon balance of the ecosystem (Sabater et al., 2016).

It should be noted that the biofilms’ CR achieved stability to the control after 10 days of rewetting. However, at the end of the rewetting, the GPP continued to increase to the control level but did not achieve stability, regardless of the duration of desiccation. It indicated that GPP is strongly inhibited in desiccation, although the resilience of GPP is higher, it still needs a long recovery time. This should be the focus of our subsequent experimental studies to determine the recovery time and the final state of GPP.

4.2 Response patterns of biofilm carbon metabolism

Since the ecological indicators such as GPP, CR, and AI only reflect the integrated functions of biofilms, the carbon metabolic activity determined by Biolog EcoPlate provides more detailed information about the dynamic responses of biofilm metabolism to dry and wet stress. During desiccation, the value of total AWCD decreased significantly on the first day and then remained at the control level (Figure 5a). After the complete drought of biofilms, the total AWCD began to decrease, while high potential carbon metabolism was observed after 25 and 90 days of desiccation. This phenomenon may be due to the existence of functional redundancy taxa in biofilm communities. Several studies have found the high potential activity of enzymes during desiccation (Pohlon et al., 2018, Su et al., 2020). This high potential activity increases during

desiccation, probably due to the continuous production of enzymes, or because the turnover rate slows down (Acuña et al., 2015).

In this study, the length of the non-flow period resulted in different responses of carbon metabolism in biofilms to flow recovery. After flow recovery, the biofilm from different non-flow periods exhibited a similar response pattern, while the recovery rate of carbon metabolism was slower after 90 days of desiccation. And the total AWCD was still below the control level at the end of the rewetting (Figure 5d,g). This suggests that prolonged desiccation has irreversible effects on carbon metabolism in biofilms. According to the response trends of different carbon sources during rewetting, with the increase of desiccation, the response trends of all carbon sources metabolism are gradually unified, which means that long-term desiccation may reduce the existence of functional redundancy taxa, and the microorganism can recover from the damaged state.

Meanwhile, the metabolism of amine and amino acid carbon sources has always shown a different trend from that of the total metabolism. In addition, enzymes might already be available when favorable conditions occur and are useful for rapid metabolism recovery in the initial phase of rewetting. Carbon metabolism thus manifests itself as ‘stress recovery’, i.e., higher than the control state and tended to over-compensate for their desiccation losses at the beginning of rewetting (Pohlon et al., 2018). Previous study found that contrary to the activities of other enzymes, the phenylalanine (amino acids) activity increased with increasing dryness (Gionchetta et al., 2020). Therefore, we speculated that this may be the reason behind our results, which show that only amino acid metabolic does not show ‘stress recovery’ at the initial stage of rewetting.

From the point of the diversity of carbon metabolism, it can also be found that the time of desiccation has significantly different effects on the metabolic function of biofilms (Fasching et al., 2020). Rewetting after short-term desiccation can restore the carbon metabolism function of biofilms in terms of activity and diversity (Figure 6). However, long-term desiccation has irreversible effects, and even the recovery of water flow after long-term desiccation is an interference with the arid system, which will further damage instead of recovery for biofilm metabolism (Datry et al., 2018 , Ge et al., 2018).

4.3 Environmental implication

According to the results of the present study, different response patterns were observed with the alternation of desiccation and rewetting of biofilms metabolism (GPP, CR, AI, and carbon metabolism). During desiccation, the ecosystem metabolism of biofilms (PR ratio) was inhibited due to the different resistance mechanisms of CR and GPP. In addition, we found that after 90 days of prolonged desiccation, ecosystem metabolism could not recover stabilizable to the control level within 20 days of rewetting (Figure 4b,c). And the total carbon metabolism of biofilm was not recovered to the control level after long-term (90 days) desiccation, suggesting that long-term desiccation and short-term desiccation have different effects on the carbon metabolism function of IRES ecosystem. In addition, some carbon source categories, amine and amino acid, have different response modes to rewetting response (Figure 5), indicating the selectivity of carbon metabolism in biofilms, which have important effects on the carbon biogeochemistry cycle of IRES.

These results provide some new insights for international decision-making on the restoration of ecological flows in IRES. From the perspective of the integrated function index and carbon metabolism, the ecological restoration of IRES should consider all river function indicators and select at least some important functional indexes based on the local ecological functions of IRES. Due to the different recovery times and degree of various biofilm functional indicators, to ensure the recovery of the overall ecological function of IRES, the index requiring a longer recovery time should be taken into consideration first.

5 Conclusions

In this study, the effects of duration of the non-flow period on the dynamic responses of biofilm metabolism to flow recovery were investigated. Based on the results, the following main conclusion were suggested:

1. The biofilm was completely dehydrated 10 days after desiccation, and the potential carbon metabolism of the biofilm remained highly active until the complete dehydration.
2. Most of the functional index of biofilms from the short-term desiccation treatments (25 days) were recovered to that of the control level after 20 days of rewetting.
3. The ecosystem metabolism and carbon metabolism of biofilms can not be restored to the control level after 90 days of desiccation, indicating that prolonged desiccation causes irreparable damage to the metabolic function of the biofilm.
4. Some carbon source categories, amine and amino acid showed different response modes to rewetting, indicating the selectivity of carbon metabolism in biofilms, which had important effects on the carbon biogeochemistry cycle of IRES.
5. In order to ensure the recovery of IRES's overall ecological function, the index requiring a longer recovery time should be taken into consideration first.

Data Availability Statement

All the data in this study has been uploaded as supplements for review purposes.

Acknowledgement

We are grateful for the grants for Project supported by the National Natural Science Foundation of China (No.51979075, and No. 52039003), the Fundamental Research Funds for the Central Universities (No. B210202053) and Jiangsu Province “333” project.

References

Acuña, V., Casellas, M., Corcoll, N., Timoner, X., Sabater, S., Naturvetenskapliga, F., . . . Gothenburg, U. (2015). Increasing extent of periods of no flow in intermittent waterways promotes heterotrophy. *Freshwater Biology*, *60*(9), 1810-1823. Retrieved from http://pku.summon.serialssolutions.com

Acuña, V., Datry, T., Marshall, J., Barceló, D., Dahm, C. N., Ginebreda, A., . . . Palmer, M. A. (2014). Why Should We Care About Temporary Waterways? *Science, 343*(6175).

Acuña, V., Wolf, A., Uehlinger, U., & Tockner, K. (2008). Temperature dependence of stream benthic respiration in an Alpine river network under global warming. *Freshwater Biology*, *53*(10), 2076-2088. doi:10.1111/J.1365-2427.2008.02028.X

Adyel, T. M., Hipsey, M. R., & Oldham, C. E. (2017). Temporal dynamics of stormwater nutrient attenuation of an urban constructed wetland experiencing summer low flows and macrophyte senescence. *Ecological Engineering, 102*, 641-661. doi:10.1016/J.ECOLENG.2016.12.026

Ahlmann-Eltze, C. (2019). Significance Brackets for 'ggplot2' [R package ggsignif version 0.6.0]. In.

Battin, T. J., Besemer, K., Bengtsson, M. M., Romani, A. M., & Packmann, A. I. (2016). The ecology and biogeochemistry of stream biofilms. *Nature Reviews Microbiology, 14*(4), 251-263. Retrieved from http://www.nature.com/articles/nrmicro.2016.15

Bogan, M. T., Chester, E. T., Datry, T., Murphy, A. L., Robson, B. J., Ruhi, A., . . . Whitney, J. E. (2017). Resistance, resilience and community recovery in intermittent rivers and ephemeral streams. In (pp. 349-376).

Bott, T. L., Brock, J. T., Baatrup-Pedersen, A., Chambers, P. A., Dodds, W. K., Himbeault, K. T., . . . Wolfaardt, G. M. (1997). An evaluation of techniques for measuring periphyton metabolism in chambers. *canadian journal of fisheries and aquatic sciences, 54*(3), 715-725. doi:10.1139/F96-323

Colls, M., Timoner, X., Font, C., Sabater, S., & Acuña, V. (2019). Effects of Duration, Frequency, and Severity of the Non-flow Period on Stream Biofilm Metabolism. *Ecosystems, 22*(6), 1393-1405. Retrieved from http://link.springer.com/10.1007/s10021-019-00345-1

Datry, T., Foulquier, A., Corti, R., von Schiller, D., Tockner, K., Mendoza-Lera, C., . . . Zoppini, A. (2018). A global analysis of terrestrial plant litter dynamics in non-perennial waterways. *Nature Geoscience, 11*(7), 497-503. Retrieved from http://www.nature.com/articles/s41561-018-0134-4

Delgado, C., Almeida, S. F. P., Elias, C. L., Ferreira, V., & Canhoto, C. (2017). Response of biofilm growth to experimental warming in a temperate stream. *Ecohydrology, 10*(6), e1868. Retrieved from https://onlinelibrary.wiley.com/doi/10.1002/eco.1868

Fabian, J., Zlatanović, S., Mutz, M., Grossart, H.-P., van Geldern, R., Ulrich, A., . . . Premke, K. (2018). Environmental Control on Microbial Turnover of Leaf Carbon in Streams – Ecological Function of Phototrophic-Heterotrophic Interactions. *Frontiers in Microbiology, 9*. Retrieved from https://www.frontiersin.org/article/10.3389/fmicb.2018.01044/full

Fan, K., Delgado-Baquerizo, M., Guo, X., Wang, D., Zhu, Y.-g., & Chu, H. (2021). Biodiversity of key-stone phylotypes determines crop production in a 4-decade fertilization experiment. *The ISME Journal, 15*(2), 550-561. Retrieved from http://www.nature.com/articles/s41396-020-00796-8

Fasching, C., Akotoye, C., Bižić, M., Fonvielle, J., Ionescu, D., Mathavarajah, S., . . . Xenopoulos, M. A. (2020). Linking stream microbial community functional genes to dissolved organic matter and inorganic nutrients. *Limnology and Oceanography, 65*(S1). Retrieved from https://onlinelibrary.wiley.com/doi/10.1002/lno.11356

Fazi, S., Vázquez, E., Casamayor, E. O., Amalfitano, S., Butturini, A., & Smidt, H. (2013). Stream hydrological fragmentation drives bacterioplankton community composition. *PloS one, 8*(5), e64109-e64109. Retrieved from http://pku.summon.serialssolutions.com

Feng, L., He, L., Jiang, S., Chen, J., Zhou, C., Qian, Z.-J., . . . Li, C. (2020). Investigating the composition and distribution of microplastics surface biofilms in coral areas. *Chemosphere, 252*, 126565. Retrieved from https://linkinghub.elsevier.com/retrieve/pii/S004565352030758X

Ge, Z., Du, H., Gao, Y., & Qiu, W. (2018). Analysis on Metabolic Functions of Stored Rice Microbial Communities by BIOLOG ECO Microplates. *Frontiers in Microbiology, 9*. Retrieved from https://www.frontiersin.org/article/10.3389/fmicb.2018.01375/full

Gionchetta, G., Artigas, J., Arias Real, R., Oliva, F., & Romaní, A. M. (2020). Multi - model assessment of hydrological and environmental impacts on streambed microbes in Mediterranean catchments. *Environmental Microbiology, 22*(6), 2213-2229. Retrieved from https://onlinelibrary.wiley.com/doi/10.1111/1462-2920.14990

Gionchetta, G., Romaní, A. M., Oliva, F., & Artigas, J. (2019). Distinct responses from bacterial, archaeal and fungal streambed communities to severe hydrological disturbances. *Scientific Reports, 9*(1). Retrieved from http://www.nature.com/articles/s41598-019-49832-4

Gómez-Gener, L., Obrador, B., Marcé, R., Acuña, V., Catalán, N., Casas-Ruiz, J. P., . . . von Schiller, D. (2016). When Water Vanishes: Magnitude and Regulation of Carbon Dioxide Emissions from Dry Temporary Streams. *Ecosystems, 19*(4), 710-723. Retrieved from http://link.springer.com/10.1007/s10021-016-9963-4

Hou, J., Li, T., Miao, L., You, G., Xu, Y., & Liu, S. (2019). Effects of titanium dioxide nanoparticles on algal and bacterial communities in periphytic biofilms. *Environmental Pollution, 251*, 407-414. Retrieved from https://linkinghub.elsevier.com/retrieve/pii/S0269749119302982

Kassambara, A. (2020). 'ggplot2' Based Publication Ready Plots [R package ggpubr version 0.4.0]. In.

Liao, K., Bai, Y., Huo, Y., Jian, Z., Hu, W., Zhao, C., & Qu, J. (2018). Integrating microbial biomass, composition and function to discern the level of anthropogenic activity in a river ecosystem. *Environment International, 116*, 147-155. Retrieved from https://linkinghub.elsevier.com/retrieve/pii/S016041201732086X

Liao, K., Bai, Y., Huo, Y., Jian, Z., Hu, W., Zhao, C., & Qu, J. (2019). Use of convertible flow cells to simulate the impacts of anthropogenic activities on river biofilm bacterial communities. *Science of The Total Environment, 653*, 148-156. Retrieved from https://linkinghub.elsevier.com/retrieve/pii/S0048969718342621

Liu, S., Wang, C., Hou, J., Wang, P., & Miao, L. (2020). Effects of Ag NPs on denitrification in suspended sediments via inhibiting microbial electron behaviors. *Water Research, 171*, 115436. Retrieved from https://linkinghub.elsevier.com/retrieve/pii/S0043135419312138

Lv, T., Carvalho, P. N., Zhang, L., Zhang, Y., Button, M., Arias, C. A., . . . Brix, H. (2017). Functionality of microbial communities in constructed wetlands used for pesticide remediation: Influence of system design and sampling strategy. *Water Research, 110*, 241-251. Retrieved from https://linkinghub.elsevier.com/retrieve/pii/S0043135416309617

Messager, M. L., Lehner, B., Cockburn, C., Lamouroux, N., Pella, H., Snelder, T., . . . Datry, T. (2021). Global prevalence of non-perennial rivers and streams. *Nature, 594*(7863), 391-397. Retrieved from http://www.nature.com/articles/s41586-021-03565-5

Miao, L., Guo, S., Liu, Z., Liu, S., You, G., Qu, H., & Hou, J. (2019). Effects of Nanoplastics on Freshwater Biofilm Microbial Metabolic Functions as Determined by BIOLOG ECO Microplates. *International journal of environmental research and public health, 16*(23), 4639. Retrieved from http://pku.summon.serialssolutions.com

Miao, L., Wang, C., Adyel, T. M., Wu, J., Liu, Z., You, G., . . . Hou, J. (2020). Microbial carbon metabolic functions of biofilms on plastic debris influenced by the substrate types and environmental factors. *Environment International, 143*, 106007. Retrieved from https://linkinghub.elsevier.com/retrieve/pii/S0160412020319620

Miao, L., Yu, Y., Adyel, T. M., Wang, C., Liu, Z., Liu, S., . . . Hou, J. (2021). Distinct microbial metabolic activities of biofilms colonizing microplastics in three freshwater ecosystems. *Journal of Hazardous Materials, 403*, 123577-123577. Retrieved from http://pku.summon.serialssolutions.com

Muñoz, I., Abril, M., Casas-Ruiz, J. P., Casellas, M., Gómez-Gener, L., Marcé, R., . . . Acuña, V. (2018). Does the severity of non-flow periods influence ecosystem structure and function of temporary streams? A mesocosm study. *Freshwater Biology, 63*(7), 613-625. Retrieved from https://onlinelibrary.wiley.com/doi/10.1111/fwb.13098

Navarro-Ortega, A., Acuña, V., Bellin, A., Burek, P., Cassiani, G., Choukr-Allah, R., . . . Barceló, D. (2015). Managing the effects of multiple stressors on aquatic ecosystems under water scarcity. The GLOBAQUA project. *Science of The Total Environment, 503-504*, 3-9. Retrieved from https://linkinghub.elsevier.com/retrieve/pii/S0048969714009541

Oksanen, J., Blanchet, F. G., Kindt, R., Legendre, P., Minchin, P. R., O'Hara, R. B., . . . Wagner, H. (2012). vegan: Community Ecology Package. In.

Pohlon, E., Rütz, N. K., Ekschmitt, K., & Marxsen, J. (2018). Recovery dynamics of prokaryotes and extracellular enzymes during sediment rewetting after desiccation. *Hydrobiologia, 820*(1), 255-266. Retrieved from http://link.springer.com/10.1007/s10750-018-3662-4

Sabater, S., Timoner, X., Borrego, C., & Acuña, V. (2016). Stream Biofilm Responses to Flow Intermittency: From Cells to Ecosystems. *Frontiers in Environmental Science, 4*. Retrieved from http://journal.frontiersin.org/Article/10.3389/fenvs.2016.00014/abstract

Schreiber, U., Müller, J. F., Haugg, A., & Gademann, R. (2002). New type of dual-channel PAM chlorophyll fluorometer for highly sensitive water toxicity biotests. *photosynthesis research, 74*(3), 317-330. doi:10.1023/A:1021276003145

Shumilova, O., Zak, D., Datry, T., Schiller, D., Corti, R., Foulquier, A., . . . Zarfl, C. (2019). Simulating rewetting events in intermittent rivers and ephemeral streams: A global analysis of leached nutrients and organic matter. *Global Change Biology, 25*(5), 1591-1611. Retrieved from https://onlinelibrary.wiley.com/doi/10.1111/gcb.14537

Steven, B., Phillips, M. L., Belnap, J., Gallegos-Graves, L. V., Kuske, C. R., & Reed, S. C. (2021). Resistance, Resilience, and Recovery of Dryland Soil Bacterial Communities Across Multiple Disturbances. *Frontiers in Microbiology, 12*. Retrieved from https://www.frontiersin.org/articles/10.3389/fmicb.2021.648455/full

Su, X., Su, X., Zhou, G., Du, Z., Yang, S., Ni, M., . . . Deng, J. (2020). Drought accelerated recalcitrant carbon loss by changing soil aggregation and microbial communities in a subtropical forest. *soil biology & biochemistry, 148*, 107898. Retrieved from http://pku.summon.serialssolutions.com

Sun, R., Xu, Y., Wu, Y., Tang, J., Esquivel-Elizondo, S., Kerr, P. G., . . . Liu, J. (2021). Functional sustainability of nutrient accumulation by periphytic biofilm under temperature fluctuations. *Environmental technology, 42*(8), 1145-1154. Retrieved from http://pku.summon.serialssolutions.com

Timoner, X., AcuÑA, V., Von Schiller, D., & Sabater, S. (2012). Functional responses of stream biofilms to flow cessation, desiccation and rewetting. *Freshwater Biology, 57*(8), 1565-1578. Retrieved from https://onlinelibrary.wiley.com/doi/10.1111/j.1365-2427.2012.02818.x

Wickham, H. (2009). *ggplot2: Elegant Graphics for Data Analysis*.

Wu, Y., Xia, L., Yu, Z., Shabbir, S., & Kerr, P. G. (2014). In situ bioremediation of surface waters by periphytons. *Bioresource Technology, 151*, 367-372. Retrieved from https://linkinghub.elsevier.com/retrieve/pii/S0960852413016751

Yurudu, N. O. S. (2012). Study of biofilm associated bacteria on polyvinyl chloride, stainless steel and glass surfaces in a model cooling tower system with different microbiological methods. *iufs journal of biology, 71*(1), 63-76.

Zak, J. C., Willig, M. R., Moorhead, D. L., & Wildman, H. G. (1994). Functional diversity of microbial communities: A quantitative approach. *soil biology & biochemistry, 26*(9), 1101-1108. doi:10.1016/0038-0717(94)90131-7

Zlatanović, S., Fabian, J., Premke, K., & Mutz, M. (2018). Shading and sediment structure effects on stream metabolism resistance and resilience to infrequent droughts. *Science of The Total Environment, 621*, 1233-1242. Retrieved from https://linkinghub.elsevier.com/retrieve/pii/S0048969717328085

Figure 1. The alternation of desiccation and rewetting experiment time axis

Figure 2. ESEM of biofilm during alternation of desiccation and rewetting. Each image is a detailed image in the red box at the top right. D0 is day 0 of desiccation and R0 is day 0 of rewetting.

Figure 3. The value of AI (a-c) of biofilm during alternation of desiccation and rewetting. The lines at AI value 200 (a, b, and c) indicate a high proportion of heterotrophic in the biofilm. The dotted lower and upper lines indicate the range of values for the control group(b, c). The error bars indicate standard deviation between parallel samples. The albaphtical letters abc indicate significant differences between samples.

Figure 4. The ecosystem metabolism (represent by the ratio of GPP and CR, a-c) and the resistance of GPP and CR during desiccation (d), and the resilience of GPP and CR after rewetting (e). The shaded grey panels in b and c indicate control. The error bars indicate standard deviation between parallel samples. The albaphtical letters abc indicate significant differences between samples.

Figure 5. The total AWCD of biofilm (a, d, g) and specific carbon sources that differ from the overall pattern of metabolism (b, c, e, f, h, i) during the alternation of desiccation and rewetting. Linerar fits of control data (a, b, c) indicate 95% confidential level. The shaded grey panels (d, e, f, g, h, i) indicate control. The error bars indicate standard deviation between parallel samples. The albaphtical letters abc indicate significant differences between samples.

Figure 6. Non-metric multidimensional scaling (NMDS) of all carbon sources (n=31) across experimental stages (Control, Desiccation, 25-Rewetting, 90-Rewetting) (a). Functional diversity of biofilms as the Shannon-wiener index (b) across the experimental stages (* $p < 0.05$, ** $p < 0.01$).